Chapter 5

Effect of sitagliptin, melatonin and combination treatment on High Fat Diet (HFD)-induced T2D mouse model

5.1 Introduction

Lifestyle changes, principally, calorie-rich diet intake and nocturnality contribute to increasing number of metabolic disorders, including obesity and Type 2 Diabetes (T2D) (Reutrakul et al., 2013). Disturbances in circadian rhythm are associated with metabolic dysregulation and glucose intolerance in humans (Scheer et al., 2009). T2D is characterized by insulin resistance, hyperinsulinemia, hyperleptinemia, oxidative stress, inflammation, metabolic and mitochondrial dysfunction. Impaired insulin action leads to hyperglycemia and dyslipidemia, which causes gluco-lipotoxicity to various cells, including pancreatic β-cells, further contributing to a reduction in β-cell mass and function (Lin et al., 2010). The prevalence of T2D is rapidly increasing worldwide. Researchers are coming up with many novel therapeutic approaches including incretin-based therapies that could suppress diabetic manifestations in different organs besides increasing β-cell mass.

Melatonin, a hormone of darkness, is known to reduce obesity and T2D (Pan et al., 2006; Peshchke et al., 2008; Stumpf et al., 2009) by regulating glucose metabolism (Peschke and Muhlbauer, 2010) and lipid metabolism (Rios-Lugo et al., 2010; Nduhirabandi et al., 2011) in both rodents and humans. When produced locally in several tissues, including the pancreas, melatonin acts as a free radical scavenger, a potent antioxidant and anti-inflammatory molecule (Galano et al., 2011; Korkmaz et al., 2009). It also has the potential to increase β-cell mass by proliferation/regeneration (Kanter et al., 2006). Pinealectomy leads to loss of melatonin which further causes hyperinsulinemia as melatonin keeps a check on insulin secretion (Nishida et al., 2003). It is shown that chronic administration of melatonin reduces insulin resistance and improves lipid metabolism in T2D rats (Nishida et al., 2002). Melatonin levels are reduced in Goto Kakizaki rats and T2D patients while they have hyperinsulinemia (Peschke et al., 2006). Recently, our study (Patel et al., 2018), along with other genome-wide association studies (GWAS) (Prokopenko et al., 2009; Bouatia-Naji et al., 2009), have shown that a variant of *melatonin receptor 1B* (*MTNR1B*) is associated with impaired FBG and T2D.

Sitagliptin, a dipeptidyl peptidase- IV (DPP-IV) inhibitor, is a second line drug for managing T2D. The therapeutic potential of sitagliptin has been assessed in various pre-clinical and clinical studies. It has been shown to reduce HbA1c and fasting blood glucose (FBG) in humans (Sakura et al., 2016). It enhances GLP-1 levels by two to three-fold following a meal (Herman et al., 2006). Sitagliptin preserves β-cell mass and function in T2D rodent model

(Mu et al., 2006, Mu et al., 2009). Further, it also reduces inflammation in islets and adipose tissue of obese mice (Dobrian et al., 2011).

Hence, we aimed to investigate the therapeutic potential of melatonin combined with sitagliptin in the amelioration of T2D manifestations in high-fat diet (HFD) induced T2D.

5.2 Materials and Methods

5.2.1 Animals

Forty young (6-8 weeks old) C57BL/6J male mice were procured from Advanced Centre for Treatment, Research and Education in Cancer (ACTREC), Navi-Mumbai, India. The animals were maintained on a 12hr light-dark cycle starting at 7:00 AM. Food and water were provided *ad libitum*. All the experimental procedures were performed according to the Purpose of Control and Supervision of Experiments on Animals (CPCSEA) guidelines which were approved by the Institutional Animal Ethical Committee (IAEC) (MSU/BC/13/2017).

5.2.2 Development of Diet-Induced Obese T2D Mouse Model and Drug Treatment

Thirty-two mice were fed with HFD for 25 weeks to develop a fully insulin-resistant Diet-Induced Obese (DIO) T2D mouse model. Simultaneously, eight mice were provided with a standard chow diet (NCD) for 25 weeks represented as NCD/control group. FBG was measured in mice after 6 hours fasting by tail snipping method using a Glucometer (TRUEresult, NIPRO Diagnostics, Pune, MH, India). Once the HFD fed mice turned diabetic (FBG>200mg/dL), mice were randomly divided into four groups: 1) HFD, 2) Sitagliptin (S) treated, 3) Melatonin (M) treated and 4) S+M treated. Melatonin (Sigma, St. Louis, MO, USA) was administered between 6 PM to 7 PM daily at a dose of 10 mg/kg BW i.p. dissolved in 0.1% ethanol and 0.9% saline. Sitagliptin (Januvia) (Merck & Co., Kenilworth, NJ, USA) was purchased in 100 mg tablets and was given at a dose of 5 g/kg diet. The drug treatment was given for four weeks. FBG levels and BW were recorded twice a week. Food and water intake were also monitored weekly.

5.2.3 Glucose Tolerance Test and Insulin Tolerance Test

The intraperitoneal glucose tolerance test (IPGTT) and intraperitoneal insulin tolerance test (IPITT) were performed post drug-treatment. For IPGTT and IPITT, all mice were fasted for 6 hours and were injected with glucose (2 g/kg BW, i.p.) and insulin (0.75 U/kg BW, i.p.),

respectively. Blood glucose levels were measured immediately at 0, 15, 30, 90, and 120 minutes by tail snipping. The total area under the curve (AUC) was calculated.

5.2.4 Metabolic and Biochemical Parameters

Before sacrificing mice, 1-2 ml blood from the orbital sinus was collected in K3 EDTA tubes and centrifuged at 6000 g for 5 minutes. Plasma was separated and stored at -20 °C for further analysis. Fasting plasma insulin, leptin and melatonin levels were estimated by commercially available mouse insulin, leptin (both from RayBiotech, GA, USA), and melatonin (Elabscience, Houston, TX, USA, Cat# E-EL-M0788) ELISA kits. Lipid profile (triglycerides, total cholesterol, HDL-c) was estimated by commercially available kits (Reckon Diagnostics Pvt. Ltd., Vadodara, GJ, India). Friedewald's (1972) formula was used for calculating low-density lipoprotein (LDL) levels.

5.2.5 Gene Expression Analysis

Liver, skeletal muscle, and adipose tissue were harvested post euthanisation and stored in RNAlater™ Stabilization Solution (Thermo Fisher Scientific, Waltham, MA, USA) for gene expression analysis. Total RNA was isolated by Trizol method. RNA integrity and purity were checked by 1.5% agarose gel electrophoresis/ethidium bromide staining and 260/280 absorbance ratio of 1.9, respectively. To avoid DNA contamination, RNA was treated with DNase I (Puregene, Genetix Biotech) before cDNA synthesis. Transcriptor High Fidelity cDNA Synthesis Kit (Roche Diagnostic GmbH, Mannheim, Germany) was used to prepare cDNA using one microgram of total RNA isolated, according to the manufacturer's instructions in the Eppendorf Mastercycler gradient (USA Scientific, Inc., Florida, USA). Transcript analysis was carried out for the key genes involved in glucoregulation (liver), mitochondrial biogenesis (skeletal muscle) and lipid metabolism (adipose tissue). *GAPDH* was used as a reference gene. Real-time PCR was performed using Light-Cycler® 480 SYBR Green I Master (Roche Diagnostics GmbH, Mannheim, Germany) and gene-specific primers (Eurofins, Bengaluru, KA India), and was carried out in the Light-Cycler® 480 Real-Time PCR (Roche Diagnostics GmbH, Mannheim, Germany). The forward and reverse primer (5'-3') details for gene expression study are as follows: *Glucokinase* (*GCK*), FP: AGGAGGCCAGTGTAAAGATGT and RP: TCCCAGGTCTAAGGAGAGAAA; *Fructose-bisphosphatase 1* (*FBP1*), FP: GCATCGCACAGCTCTATGGT and RP: CTCAGGTTCGATTATGATGGC; *Phosphoenolpyruvate carboxykinase* (*PEPCK*), FP: CTGCATAACGGTCTGGACTTC and RP: CAGCAACTGCCCGTACTCC; *Glucose-6-*

phosphatase (*G6Pase*), FP: CTGTTTGGACAACGCCCGTAT and RP: AGGTGACAGGGAACTGCTTTA; *Glucose transporter 2* (*GLUT2*), FP: CTTGGAAGGATCAAAGCAATG and RP: CAGTCCTGAAATTAGCCCAC; *Glycogen synthase* (*GS*), FP: ACCAAGGCCAAAACGACAG and RP: GGGCTCACATTGTTCTACTTG; *Glycogen phosphorylase* (*GP*), FP: GAGAAGCGACGGCAGATCA and RP: CTTGACCAGAGTGAAGTGCA; *Sirtuin 1* (*SIRT1*), FP: GATGAAGTTGACCTCCTCA and RP: GGGTATAGAACTTGGAATTAG; *Peroxisome proliferator-activated receptor gamma coactivator 1-alpha* (*PGC1-α*), FP: AGCCGTGACCACTGACAACGA and RP:GTAGCTGAGCTGAGTGTTGGC; *Acetyl-CoA carboxylase* 1 (*ACC1*), FP: ACGCTCAGGTCACCAAAAAGAAT and RP: GTAGGGTCCCGGCCACAT; *Adipose triglyceride lipase* (*ATGL*), FP: CAACGCCACTCACATCTACGG and RP: GGACACCTCAATAATGTTGGCAC; *GAPDH*, FP: AGGTCGGTGTGAACGGATTTG and RP: TGTAGACCATGTAGTTGAGGT. Real-time PCR was performed as described previously by determining $2^{-\Delta\Delta Ct}$ (Patel et al., 2018).

5.2.6 Droplet Digital PCR (ddPCR)

Gene expression of *MTNR1B*, glucose transporter 4 (*GLUT4*), and tumor necrosis factor alpha (*TNF-α*) in mouse adipose tissue were monitored by ddPCR using EvaGreen dye (Bio-Rad, Hercules, CA, USA). Each ddPCR reaction contained 20 µl of mastermix including 10 µl of EvaGreen Supermix, 0.5 µl (2.5 mM) forward primer and reverse primer each, 1 µl cDNA (50 ng) and 8 µl nuclease free water. This system was loaded in a droplet generator cartridge along with 70 µl of droplet generation oil into oil well. QX200™ Droplet Generator was used for generating droplets and the droplets were loaded to 96 well PCR plate. The plate was heat-sealed with foil and was run in a thermal cycler. The PCR conditions for the assay were: 95 °C for 5 min; 40 cycles of 95 °C for 30s and 60 °C (depending on annealing temperature) for 1 min; and three final steps at 4 °C for 5 min, 90 °C for 5 min, and a 4 °C for 30 min to boost dye stabilization. The PCR was read in QX200™ Droplet Reader and was analyzed by QuantaSoft™ software. The results were plotted as Ch1Amplitute and copies/µl. Blue droplets show number of positive droplets for their respective target genes and grey droplets indicate negative droplets for the target genes. Non template control was run for each assay. The details of the forward and reverse primers (5'-3') for the target genes are as follows: *MTNR1B*, FP: TTGTGATGGGCCTGAGTGTC and RP:

AGCCAGACGAGGCTGATGTA; *GLUT4*, FP: TAGGAGCTGAGGGTTGGCTA and RP: TGCTCCAGTAGGCCGTAAAC; *TNF-α*, FP: CCTCACTCACAAACCACCA and RP: ACAAGGTACAACCCATCGGC.

5.2.7 Glucoregulatory Enzymes Activity and Liver Glycogen Content

The liver was harvested post euthanisation, snap freezed and stored at -80 °C for the enzyme activity assay. Liver tissue (50 mg) was homogenised, and the lysates were used for enzyme activity assays. Enzyme assays (GCK, FBPase, PEPCK and GP) and the estimation of glycogen content were carried out by commercially available kits (BioVision, Milpitas, CA, USA; Cat# K969-100, Cat# K590-100, Cat# K359-100, Cat# K179-100 and Cat# K646-100) according to the manufacturer's protocols.

5.2.8 Respiratory Control Ratio (RCR)

For RCR studies, skeletal muscle was harvested post euthanisation and stored in mitochondrial respiration buffer at -80 °C. Mitochondria were isolated from skeletal muscle using a mitochondria isolation kit (Thermo Scientific^{TM}, Cat# 89801) using the manufacturer's protocol. The isolated mitochondria were resuspended in 100 µl of mitochondria respiration buffer (110 mM Sucrose, 0.5 mM EGTA, 70 mM KCl, 0.1% FFA free BSA, 20 mM HEPES, 3 mM $MgCl_2$, and 10 mM KH_2PO_4, 20 mM Taurine) (Butterick et al., 2016). RCR studies were carried out in Oxytherm+ System (Hansatech Instruments Ltd., Pentney, UK). Mitochondrial outer membrane integrity of the isolated mitochondria was assessed by impermeability to exogenous cytochrome c, which was consistently greater than 95%. The activities of respiratory chain complexes I-IV were monitored using 100 µl of substrates [100 mM Pyruvate & 800 mM Malate (complex I), 1 M Succinate (complex II), 10 mM α-glycerophosphate (complex III) and 0.8 M ascorbate (complex IV)] (Li and Graham, 2012), added to 90 µl of mitochondria suspension. Other respiration reagents used were 100 mM adenosine diphosphate (100 µl), 1 mM oligomycin (2 µl), 1 mM rotenone (1 µl), and 1 mM Antimycin (2.5 µl). Protein concentration was estimated by the Bradford method (Stoscheck et al., 1990). All chemicals were purchased from Sigma-Aldrich, USA. OCR was determined by measuring the amount of oxygen (nmol) consumed, divided by the time elapsed (min) and the amount of protein present in the assay (Li and Graham, 2012). Data is represented as respiratory control ratio (RCR) of state 3/state 4 respiration.

5.2.9 Western Blot Analysis

Skeletal muscle was harvested post euthanisation and stored in lysis buffer at -80 °C for western blot analysis of key proteins involved in the insulin signalling pathway. The tissue was homogenised in liquid nitrogen and Laemmli buffer (1M Tris HCl, 10% SDS, 20% glycerol and 10% β-mercaptoethanol) containing 1 M urea (1:1), protease inhibitor cocktail, and phosphatase inhibitor cocktail 2 and 3 (both from Sigma, St. Louis, MO, USA). The homogenate was collected and sonicated twice in chilled condition and centrifuged to remove tissue/cell debris. The protein concentration in the lysates was estimated using the Bradford method (Stoscheck et al., 1990) and 25-40 µg of the lysates were resolved on 8-10% sodium dodecyl sulphate–polyacrylamide gel electrophoresis (SDS-PAGE), followed by electrophoretic transfer to PVDF membrane. Membranes were blocked with 5% bovine serum albumin (Sisco Research Laboratories Pvt. Ltd., Mumbai, MH, India) for phosphorylated proteins and 5% blotting-grade blocker for non-phosphorylated proteins (Bio-Rad, Hercules, CA, USA) in Tris-buffered saline (pH 8.0) with 0.1% Tween-20 for 1 hour at room temperature. Immunoblot analysis was done with primary antibodies at a dilution of 1:1000 targeting rabbit anti-insulin receptor β, rabbit anti-insulin receptor substrate-1 (pIRS-1) Ser307 (both from Cell Signaling Technology, Cat# 3025 and Cat# 2381), rabbit anti-IRS1, rabbit anti-pAkt1 Ser473, rabbit anti-Akt1, mouse anti-β-actin (all from ABclonal Technology; Cat# A0245, Cat# AP0140, Cat# A7270 and Cat# AC004), and rabbit anti-glucose transporter 4 (GLUT4) (Sigma, Cat#CBL243) incubated overnight at 4 °C. Blots were then incubated with goat anti-rabbit immunoglobulin G (IgG)-horseradish peroxidase (HRP) (Jackson ImmunoResearch, Cat# 111035144) or goat anti-mouse IgG-HRP (Genei, Cat# 105502) at 1:5000 – 1:10,000 dilution for one hour at room temperature. The membranes were visualised with clarity western ECL substrate (Bio-Rad Laboratories, USA) in the ChemiDoc™ Touch Imaging System. Blots were analysed in Image Lab™ software (Bio-Rad Laboratories, USA).

5.2.10 Immunohistochemistry-Immunofluorescence (IHC-IF)

Pancreas was harvested post euthanisation and fixed in 10% neutral buffered formalin (NBF) for histological processing and paraffin embedding. 5µm sections were cut from the paraffin-embedded blocks. Immunofluorescence staining was carried out to study β-cell mass and islet number. The sections were deparaffinised in xylene and rehydrated in a series of graded ethanol. Antigen retrieval was performed using 1N HCL for 40 minutes at 37 °C. Sections were blocked in 5% normal donkey serum (Jackson ImmunoResearch, Cat# 017-000-121) in

PBST (PBS + 0.1% Tween 20) for 1 hour at room temperature and incubated with primary antibody prepared in blocking buffer at 37 °C in a humidified chamber for 2 hours [guinea pig anti-insulin (DAKO, Cat# A0564; 1:200). Sections were washed with PBS and were incubated with secondary antibody prepared in blocking buffer at room temperature for 45 minutes in the dark [donkey anti-guinea pig Alexa Fluor 488, Jackson ImmunoResearch, Cat# 706-545-148; 1:500]. Sections were washed with PBS and distilled water and were mounted with Slowfade® Gold Antifade mountant with DAPI (Thermo Fisher Scientific, USA), and the coverslips were sealed with nail varnish. Stained sections were observed under a confocal laser scanning microscope (Olympus FV10i, Tokyo, Japan). Image analysis was carried out in Image J software. Observations were made from three pancreatic sections per group from five different areas. β-cell mass (mg/pancreas) was calculated as (% insulin-positive area/ total insulin-positive area) x pancreas weight.

5.2.11 Statistical Analyses

All results were confirmed in at least three independent experiments for the *in-vitro* study. Statistical comparisons of data were performed by one-way analysis of variance (ANOVA) and multiple group comparisons by Tukey's post hoc test in Prism 5 (GraphPad Sofware, San Diego, CA, USA). The significance level was set as $p<0.05$. Results are expressed as mean±SEM.

5.3 Results

5.3.1 Development of Diet-Induced Obese T2D Mouse Model

Diet-induced obese (DIO) mouse T2D model was developed after 25 weeks of HFD feeding in C57BL/6J male mice. BW and FBG were measured once a week up to twenty-five weeks of HFD feeding for the model generation. Our data suggested that BW and FBG started increasing from 16th week of HFD feeding as compared to NCD. FBG levels were significantly increased ≥200 mg/dL at 25th week. Glucose tolerance test was carried out in the 25th week to check impaired glucose tolerance in HFD group. The results suggested that glucose tolerance was significantly reduced in HFD group as compared to NCD ($p<0.01$) along with BW and FBG levels, and a dissected open mouse shows increase in white adipose tissue indicating a successful model generation (Figure 5.1)

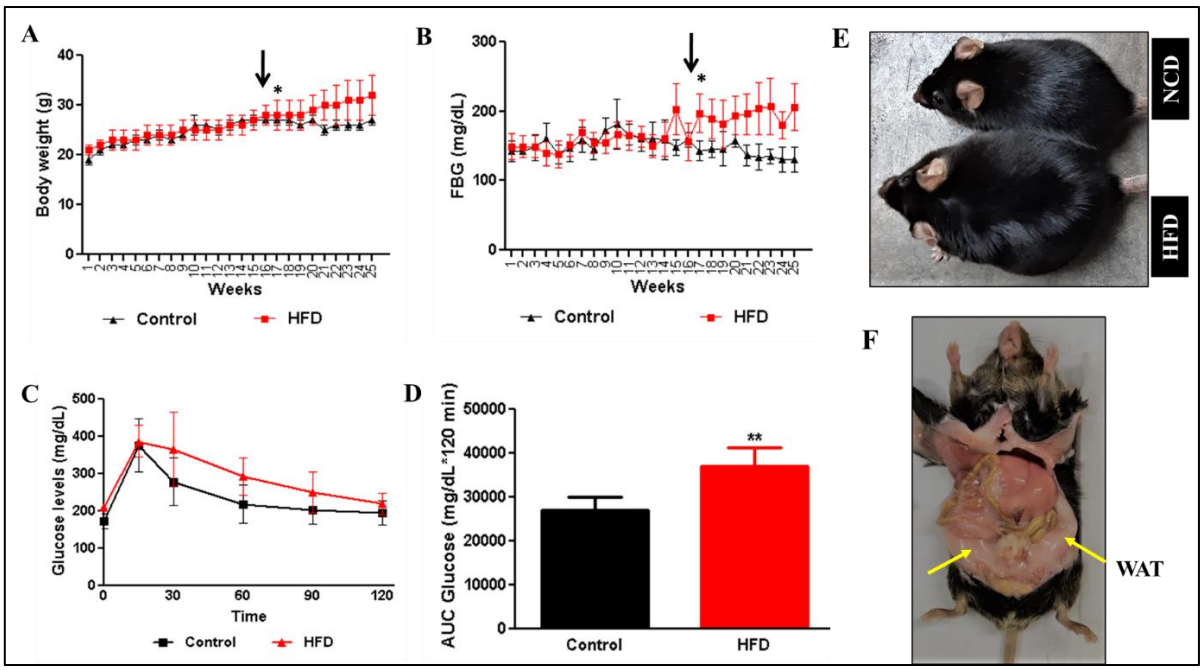

Figure 5.1 Establishment of DIO T2D mouse model: A. Body weight. HFD group showed significant increase in body weight as compared to control (NCD) at 25th week of HFD feeding. **B. Fasting blood glucose levels. HFD group showed significant increase in FBG levels (**≥200 mg/dL) at 25th week. **C-D. IPGTT and AUC curve.** Glucose tolerance was significantly reduced in HFD group as compared to control at 25th week. **E-F. Body fat mass.** HFD fed mice showed increase in white adipose tissue (WAT) (**p*<0.05, ***p*<0.01) (NCD, n=8; HFD, n=32).

5.3.2 Analysis of Metabolic Parameters

Our results suggest that HFD group showed significant increase in BW ($p<0.01$) and FBG ($p<0.01$) levels as compared to NCD. In addition, the glucose tolerance ($p<0.01$) and insulin tolerance ($p<0.05$) were also reduced in HFD group. The combination therapy revealed that its effect was greater ($p<0.001$) as compared to the monotherapies (S, $p<0.01$; M, $p<0.01$) in reducing FBG levels, increasing glucose tolerance (S, $p<0.01$; M, $p<0.05$; S+M $p<0.001$) and insulin sensitivity (S, $p>0.05$; M, $p>0.01$; S+M, $p<0.001$). The monotherapies and combination therapy did not show any significant change in the final BW compared to their initial BW ($p>0.05$). Moreover, assessment of food and water intake revealed that there was a significant reduction in food (HFD, S, M, S+M; $p<0.001$) and water intake (HFD, $p<0.001$; S, $p<0.01$; S+M; $p<0.001$) after four weeks of the drug treatment as compared to NCD group. However, the water intake was significantly higher in M group as compared to HFD group ($p<0.05$) (Figure 5.2A-F).

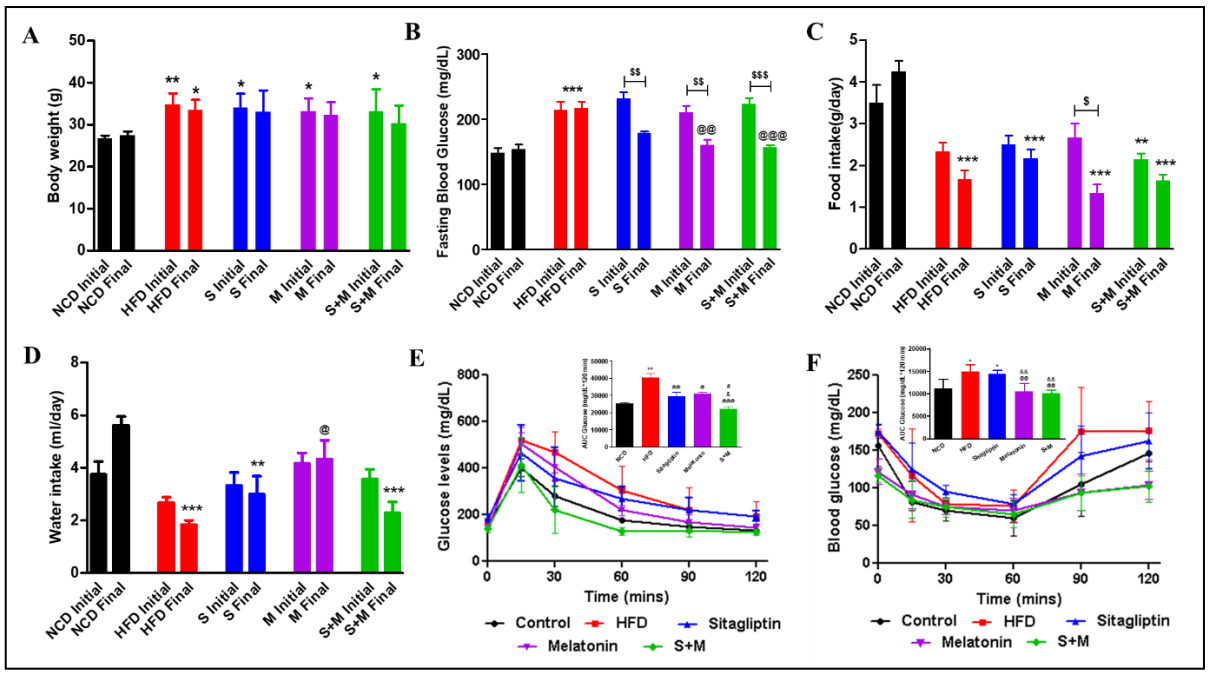

Figure 5.2 Body weight, blood glucose levels, food and water intake, IPGTT and IPITT: A. Body weight. A significant increase in body weight was observed in HFD fed mice as compared to NCD. No significant difference was observed in the body weight post drug treatment. **B. Fasting blood glucose levels.** A significant increase in FBG levels was observed in HFD fed mice and reduced in all the drug-treated groups 4 weeks post-treatment. **C. Food intake.** A significant reduction in food intake was observed in the melatonin group post-treatment, while HFD fed and other drug-treated groups showed reduction as compared to NCD. **D. Water intake.** A significant reduction in water intake was observed in HFD than in NCD, while the melatonin treated group showed a significant increase in water intake compared to HFD. **E. IPGTT.** Increased glucose clearance was observed in all the drug-treated groups as compared to HFD. **F. IPITT.** Melatonin and S+M treated groups showed significant increase in insulin sensitivity as compared to HFD. (*p<0.05, **p<0.01, ***p<0.001 vs. NCD; $^{@}p$<0.05, $^{@@}p$<0.01, $^{@@@}p$<0.001 vs. HFD; $^{\&}p$<0.05, $^{\&\&}p$<0.01, vs. Sitagliptin; $^{\#}p$<0.05 vs. Melatonin) (n=6-8/group).

5.3.3 Analysis of Plasma Lipid Profile, Insulin, Leptin and Melatonin levels

Analysis of plasma lipid profile suggested that the levels of TG, TC were increased in HFD group but were not significant, but HDL-c and LDL-c were significantly increased in HFD group (p<0.001) as compared to NCD indicating dyslipidemia. Lipid levels were restored in the monotherapies and combination-treated groups as compared to HFD group (TG and TC: S, M, S+M, p<0.05; HDL-c and LDL-c: S, M, S+M, p<0.01). Analysis of plasma insulin, leptin and melatonin levels revealed that there was hyperinsulinemia and hyperleptinemia in the HFD group as compared to NCD (p<0.01), and the levels were restored in the drug-treated groups (insulin: S, M, S+M, p<0.05; leptin: S+M, p<0.05) as compared to HFD

group. There was no change observed in melatonin levels. However, it was significantly increased in the M group (p<0.05) (Figure 5.3A-G).

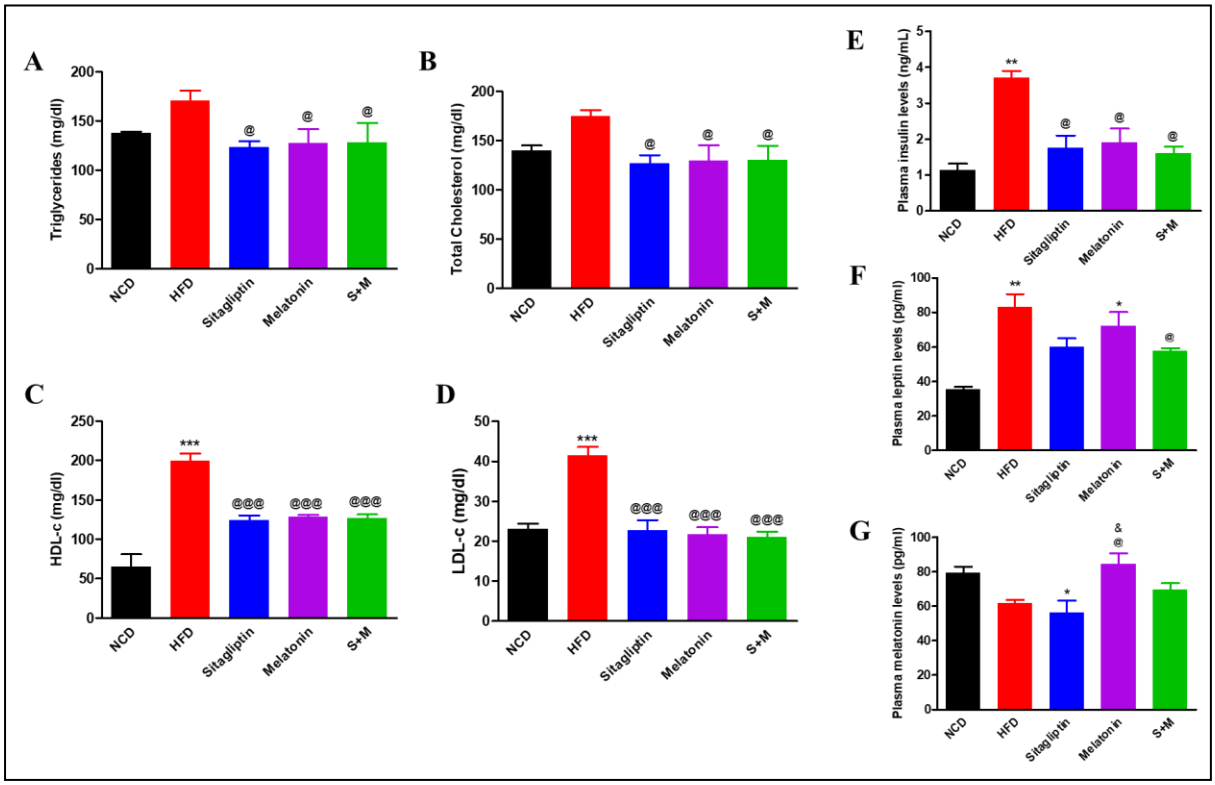

Figure 5.3 Plasma lipid profile, insulin, leptin and melatonin levels: A significant reduction of **A.** triglycerides, **B.** total cholesterol, **C.** HDL-c and **D.** LDL-c was observed in all the drug-treated groups as compared to HFD. **E. Fasting plasma insulin levels:** A significant reduction in plasma insulin was observed in the drug-treated groups as compared to HFD. **F. Fasting plasma leptin levels:** A significant reduction in plasma leptin was observed in the S+M treated group as compared to HFD. **G. Fasting plasma melatonin levels:** A significant increase in plasma melatonin was observed in the melatonin group as compared to HFD. (*p<0.05, **p<0.01 vs. NCD; $^{@}p$<0.05, $^{@@@}p$<0.001 vs. HFD; $^{\&}p$<0.05, vs. Sitagliptin) (n=6-8/group).

5.3.4 Analysis of Glucoregulatory Enzyme Activity, Liver Glycogen Content and Gene Expression

Gene expression and specific activity of glucoregulatory enzymes in the liver were monitored. The data revealed that in HFD group, *GCK* expression (p<0.05) along with FBPase expression (p<0.01) and activity (p<0.05), PEPCK expression (p<0.001) and activity (p<0.01), and GP expression (p<0.05) and activity (p<0.001) were significantly increased as compared to NCD, indicating dysregulated glucose metabolism. However, there was no change in the GCK activity (p>0.05). In addition, there was a significant reduction in *G6Pase* (p<0.001) and *GLUT2* (p<0.01) expression besides reduced liver glycogen content (p<0.001)

in HFD group as compared to NCD. With respect to the treatment groups, *GCK* expression was significantly increased in S (p<0.001), and its enzyme activity was also significantly increased in the S+M group (p<0.01) as compared to HFD group indicating increased glucose uptake. *G6Pase* was significantly reduced in S (p<0.01) and increased in M group (p<0.001), indicating increased glucose uptake while there was no change in S+M group. *GLUT2* expression was significantly reduced (S, S+M, p<0.001). Furthermore, the gene expression and activity of FBPase and PEPCK were significantly increased in the HFD group (p<0.01 and p<0.05, respectively) as compared to NCD groups, and significantly reduced in all the drug-treated groups (FBPase: S, M, S+M, p<0.05; PEPCK: S, M, S+M, p<0.01), indicating reduced gluconeogenesis. In addition, there was a significant reduction in the gene expression (S, p<0.01; M, p<0.05; S+M, p<0.001) and activity of GP (S, M, p<0.01; S+M, p<0.001) in all the drug-treated groups as compared to HFD indicating reduced glycogenolysis. The GS expression was significantly increased in the S group as compared to HFD (p<0.001) and the glycogen content in all the drug-treated groups (S, M, S+M, p<0.001), indicating an increase in glycogenesis (Figure 5.4A-L).

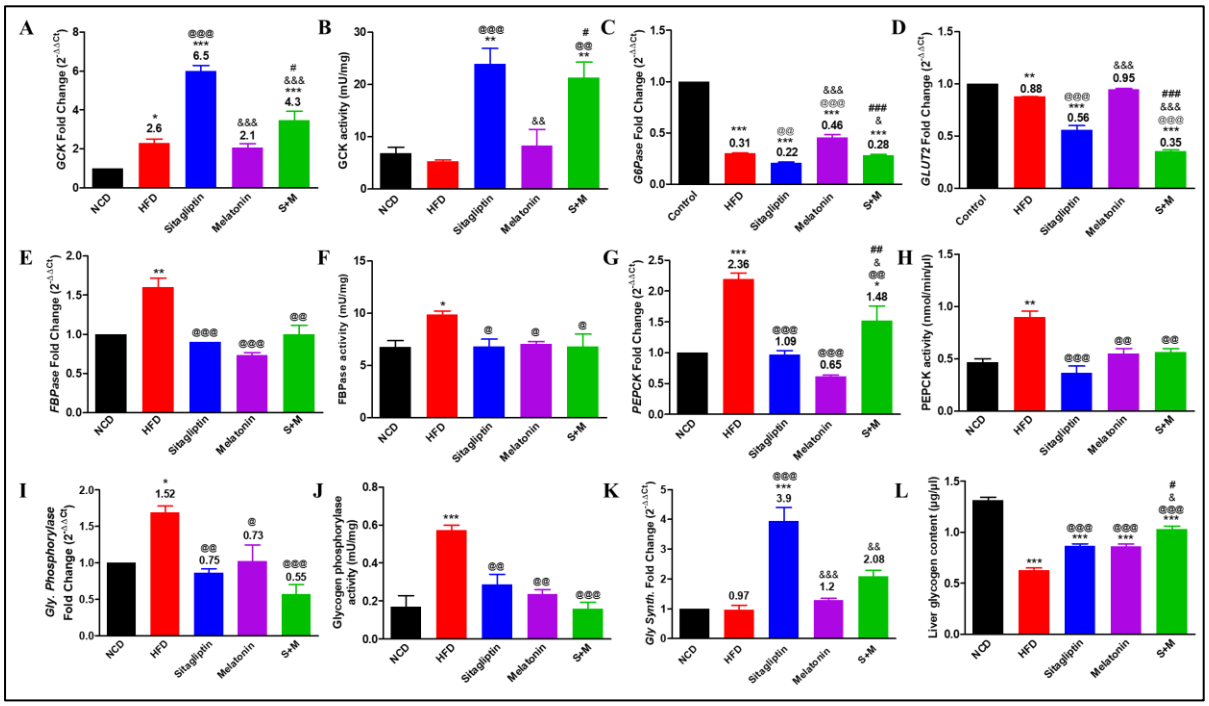

Figure 5.4 Gene expression and enzyme activities of glucoregulatory enzymes and glycogen content in the liver: A-B. GCK mRNA fold change and activity. GCK expression was significantly increased in S while its activity in S and S+M groups. **C. *G6Pase* mRNA folds change.** *G6Pase* expression was significantly decreased in S and increased in the M group. **D. *GLUT2* mRNA fold change.** A significant decrease in *GLUT2* expression was observed in the S, and S+M treated groups. **E-F. *FBPase* mRNA fold change and its activity.** *FBPase* gene expression and its activity were

significantly increased in HFD, whereas it was significantly reduced in all the drug-treated groups. **G-H. PEPCK mRNA fold change and activity.** PEPCK expression and activity were significantly reduced in all the drug-treated groups. **I-J. GP mRNA fold change and activity.** A significant decrease in GP expression and activity was observed in all the drug-treated groups. **K. *GS* mRNA fold change.** A significant increase in *GS* expression was observed in the sitagliptin treated group. **L. Liver glycogen content:** GC was significantly increased in all the drug-treated groups. (*p<0.05, **p<0.01, ***p<0.001 vs. Control; $^{@}p$<0.05, $^{@@}p$<0.01, $^{@@@}p$<0.001 vs. HFD; $^{\&}p$<0.05, $^{\&\&}p$<0.01, $^{\&\&\&}p$<0.001 vs. Sitagliptin; $^{\#}p$<0.05, $^{\#\#}p$<0.01, $^{\#\#\#}p$<0.001 vs. Melatonin) (n=6-8/group).

Furthermore, expression of *SIRT1* and *PGC1α,* which are involved in mitochondrial biogenesis pathway, showed a significant reduction in HFD group (p<0.05) as compared to NCD, while it was increased in all the drug-treated groups as compared to HFD (SIRT1: S, M, S+M, p<0.001; PGC1α: M, p<0.05, S+M, p<0.01). Lipid metabolism markers viz. *ACC1* expression was reduced in both HFD and the drug-treated groups (S, M, S+M, p<0.001) as compared to NCD with no change in the drug-treated groups (S, M, S+M, p>0.05) as compared to HFD group. *ATGL* expression was significantly increased in HFD group as compared to NCD (p<0.001), while it was significantly reduced in all the drug-treated groups (S, M, S+M, p<0.001) as compared to HFD, showing improved lipid metabolism (Figure 5.5A-D).

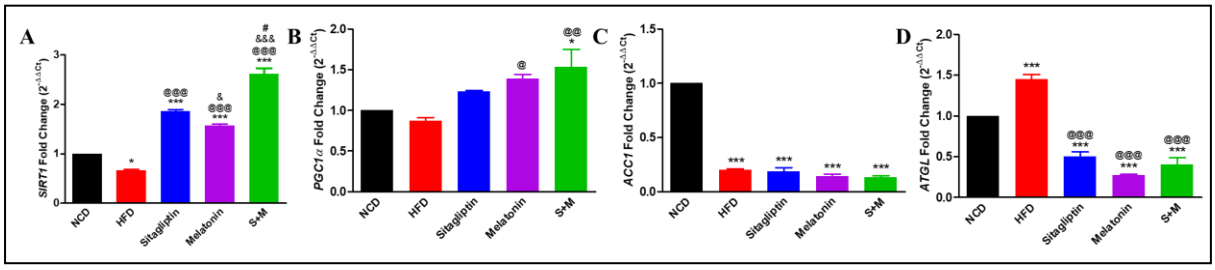

Figure 5.5 Gene expression of mitochondrial biogenesis markers in skeletal muscle and lipid metabolism markers in adipose tissue. A-B. mRNA fold change of *SIRT1* and *PGC1a* in skeletal muscle. A significant increase in *SIRT1* and *PGC1a* expression was observed in HFD (0.6-fold), whereas all the drug-treated groups showed a significant increase in *SIRT1* expression (1.8 to 2.5-fold). However, *PGC1*a expression was significantly increased only in melatonin and S+M treated groups (1.4 to 1.6-fold). **C-D. mRNA fold change of *ACC1* and *ATGL* in adipose tissue.** There was no change in *ACC1* expression, whereas a significant reduction in *ATGL* gene expression was observed in all the drug-treated groups (50 to 70%). (*p<0.05, ***p<0.001 vs. NCD; $^{@}p$<0.05, $^{@@}p$<0.01, $^{@@@}p$<0.001 vs. HFD; $^{\&}p$<0.05 vs. Sitagliptin; $^{\#}p$<0.05 vs. Melatonin) (n=6-8/group).

5.3.5 Absolute Gene Quantification of *MTNR1B, GLUT4* and *TNF-α* in Adipose Tissue

Furthermore, absolute gene expression of *MTNR1B, GLUT4*, and *TNF-α* in adipose tissue was studied by ddPCR. The results show an increased copy number/µl of the mentioned genes in the HFD group as compared to NCD group indicating higher expression and insulin

resistance. Moreover, in the treatment groups (monotherapies and combination), the copy number/µl were reduced suggesting reduced insulin resistance (Figure 5.6).

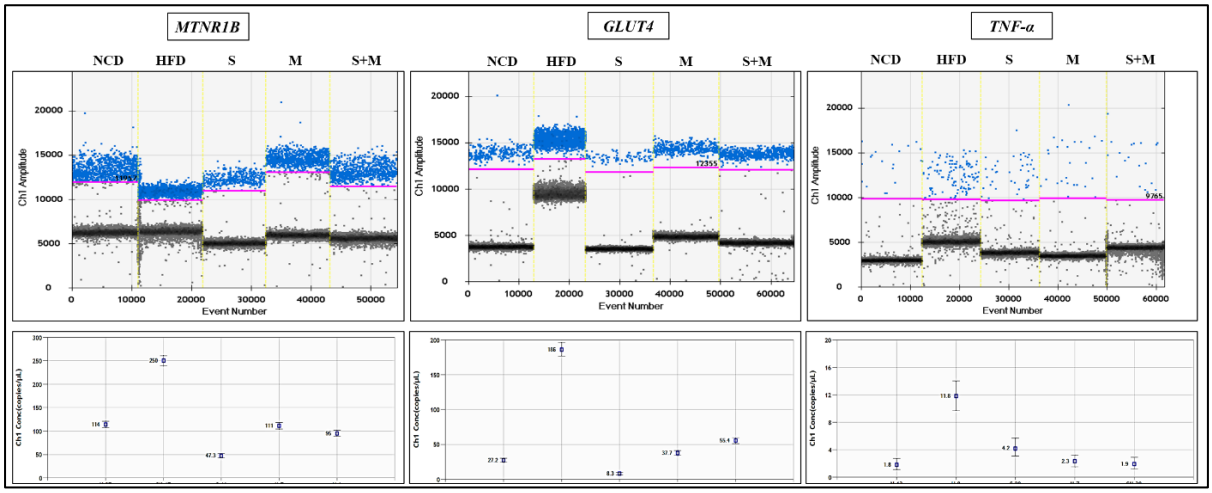

Figure 5.6 Absolute gene quantification of *MTNR1B, GLUT4,* and *TNF-α* in adipose tissue. Gene expression of *MTNR1B, GLUT4* and *TNF-α* was higher in HFD group as compared to NCD group whereas it was reduced in the all the treatment groups as compared to the HFD groups, as represented by change in amplitude of positive droplets (blue) and number of copies/µl. (n=3/group). Blue droplets: positive for the target gene; Grey droplets: negative for the target gene; Pink line: threshold intensity to discriminate positive and negative droplets.

5.3.6 Assessment of Mitochondrial Respiratory Control Ratio (RCR) of Complexes I-IV

The RCR of state 3/state 4 in the HFD group was significantly reduced as compared to NCD for the mitochondrial complexes I, II, III and IV ($p<0.001$, $p<0.05$, $p<0.05$, $p<0.001$, respectively), while a significant increase in the RCR was observed in melatonin and S+M treated groups in CII (M, $p<0.05$; S+M, $p<0.01$) CIII (M, $p<0.05$; S+M, $p<0.01$), and CIV (M, $p<0.001$; S+M, $p<0.001$). However, the RCR of state 3/state 4 in complex I was significantly increased only in the S+M ($p<0.01$) treated group (Figure 5.7A-D).

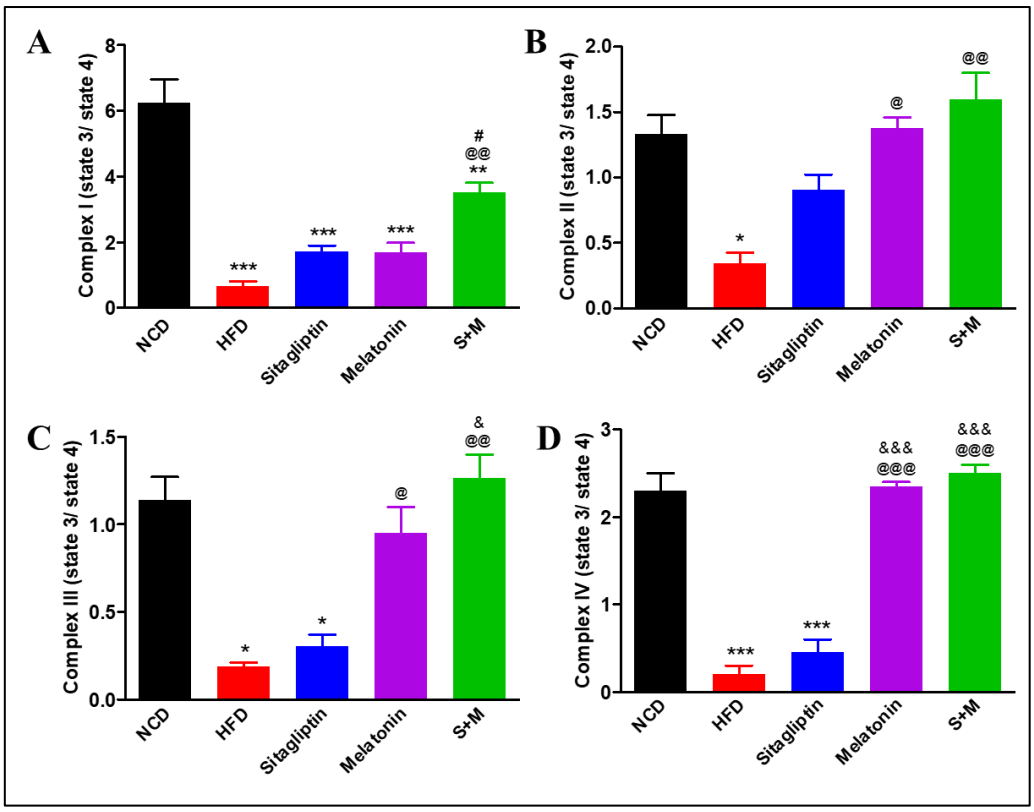

Figure 5.7 Respiratory control ratio (state 3/state 4): A) Complex I. RCR was significantly reduced in HFD group as compared to NCD and was significantly increased in the S+M treated group. **B-D) Complex II-IV.** RCR was significantly reduced in HFD group as compared to NCD and was significantly increased in the melatonin and S+M treated groups. (*p<0.05, ***p<0.001 vs. NCD; $^{@}p$<0.05, $^{@@}p$<0.01, $^{@@@}p$<0.001 vs. HFD; $^{\&}p$<0.05, $^{\&\&\&}p$<0.001 vs. Sitagliptin; $^{\#}p$<0.05, vs. Melatonin) (n=3/group).

5.3.7 Protein Expression Analysis for Insulin Signalling Pathway in Skeletal Muscle

Protein expression analysis of key proteins involved in insulin signalling pathway revealed that IR1β (p<0.001), pAkt Ser473/Akt (p<0.05) and GLUT4 (p<0.01) levels were significantly reduced in HFD fed mice while pIRS Ser307/IRS (p<0.05) was significantly increased in HFD (p<0.05) as compared to NCD, which is indicative of insulin resistance. With respect to the treatment groups, no significant change was observed in the levels of IR1β and pAkt/Akt in monotherapies (p>0.05), while a significant increase was observed in the S+M group (p<0.01, p<0.05) as compared to HFD group. Further, the levels of pIRS/IRS were significantly reduced in M and S+M groups (M, p<0.05; S+M, p<0.05) indicative of increased insulin sensitivity. Interestingly, GLUT4 levels were significantly increased in all the drug treated groups (S, p<0.001; M, p<0.01; S+M, p<0.001) as compared to HFD group. The results are shown in Figure 5.8A-D. These results indicate that the combination therapy showed significant effects as compared to monotherapies in improving insulin sensitivity.

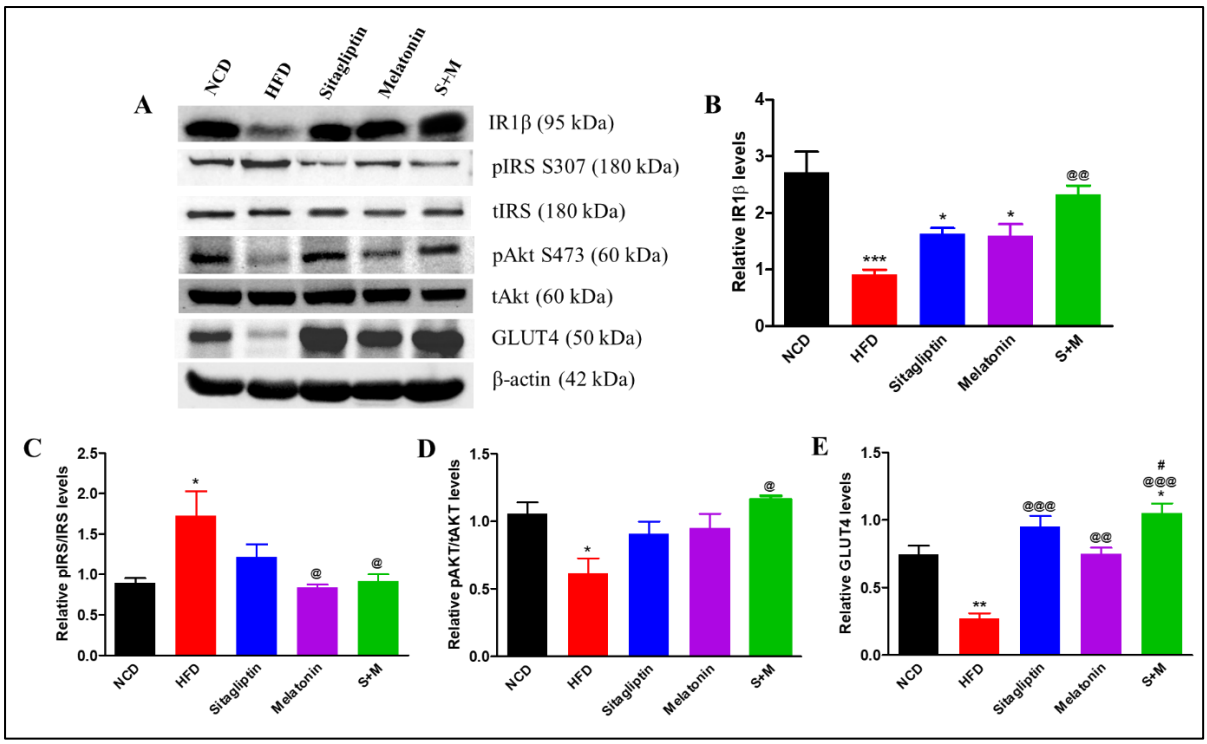

Figure 5.8 Protein expression of the insulin signalling pathway in skeletal muscle: A. Representative Western blot images. **B. Insulin Receptor 1β.** IR1β protein expression was significantly reduced in HFD compared to NCD, whereas a significant increase in IR1β was observed in S+M group. **B. pIRS/IRS.** pIRS/IRS levels were significantly increased in HFD and were significantly reduced in in M an S+M groups. **C. pAkt/Akt**. pAkt/tAkt protein expression was significantly decreased in HFD while it was significantly increased in S+M group. **D.GLUT4.** GLUT4 protein expression was significantly decreased in the HFD while it was significantly increased in all the drug treated groups. (*p<0.05, **p<0.01, ***p<0.001 vs. NCD; $^{@}p$<0.05, $^{@@}p$<0.01, $^{@@@}p$<0.001 vs. HFD; $^{\#}p$<0.05, vs. Melatonin) (n=4/group).

5.3.8 Assessment of β-cell Mass and Islet Number

Immunohistochemical analysis of the pancreas revealed that β-cell mass was significantly increased in the HFD group as compared to NCD (p<0.001). All the drug-treated groups showed significant decrease in β-cell mass as compared to HFD group (S, M, S+M, p<0.001). Interestingly, the islet number per pancreatic section was also significantly increased in HFD group (p<0.001) as compared to NCD while it was reduced in all the drug-treated groups as compared to HFD group (S, p<0.01; M, p<0.001; S+M, p<0.001), as shown in Figure 5.9A-C.

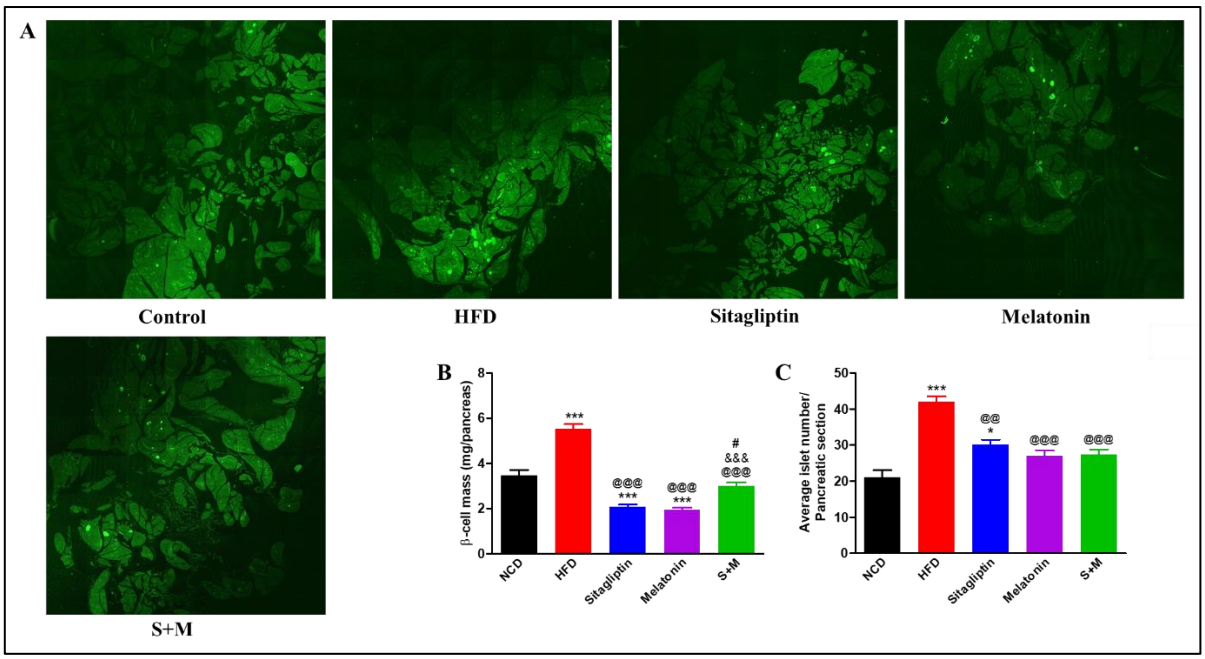

Figure 5.9 β-cell mass and Islet number. A. Immunofluorescence staining for insulin (green) in mouse pancreatic tissue. Scale- 50µm. Magnification- 60X. **B. β-cell mass in pancreas:** β-cell mass was significantly increased in HFD group while it was significantly reduced in all the drug-treated groups as compared to HFD group. **C. Number of islets per pancreatic section.** Islet number was significantly increased in HFD group as compared to NCD group while it was reduced in all the drug-treated groups as compared to HFD group (*p<0.05, ***p<0.001 vs. NCD; $^{@@}p$<0.01, $^{@@@}p$<0.001 vs. HFD; $^{\#}p$<0.05 vs. Melatonin) (n=6-8/ group).

5.4 Discussion

T2D is a metabolic disorder with a reduced incretin effect and disturbed circadian rhythm (Scheer et al., 2009). Several studies have linked genetic variants of *MTNR1B* and reduced melatonin levels with T2D pathogenesis. T2D is a multifactorial disorder involving various factors like insulin resistance, leptin resistance, metabolic and mitochondrial dysfunction, and reduced β-cell mass and function. We have shown in Chapter 4 the effect combination therapy using sitagliptin and melatonin in the amelioration of T1D in mouse model by increasing β-cell mass. Here, we aimed to study the therapeutic potential of combination therapy of sitagliptin and melatonin in the amelioration of T2D manifestations in mouse model. Our results show that sitagliptin and melatonin alone and in combination can ameliorate hyperglycemia, hyperinsulinemia, hyperleptinemia, dyslipidemia and improve glucose and lipid metabolism. In addition, it preserves β-cell mass and islet number, increases mitochondrial biogenesis, and insulin sensitivity in skeletal muscle and adipose tissue.

Apart from the pineal gland, melatonin is locally synthesized in various tissues like retina, pancreas, adipose tissue, etc. This pleiotropic hormone mediates its action via MTNR1A and MTNR1B receptors in central and peripheral tissues, regulating metabolic functions. These receptors are G protein-coupled receptors, and most of the signalling pathways are dependent on Gi proteins, which inhibit protein kinase A (PKA) - cAMP response element-binding protein (CREB) pathway. Gi proteins also inhibit other kinases such as protein kinase G (PKG), protein kinase C (PKC), phosphoinositide 3-kinase (PI3K), Akt, extracellular-signal-regulated kinase (ERK) and ion channels such as Kir3 and large-conductance Ca^{2+}-activated potassium channels (BKCa) (Cecon et al., 2017). Alternatively, melatonin activates Gq-PKC-phospholipase C (PLC) pathway, which is shown to stimulate insulin secretion (Oishi et al., 2018). A few animal studies suggest modulatory effects of melatonin in peripheral tissues even though melatonin receptors are expressed at low levels in these tissues (Ha et al., 2006; Poon et al., 2001; Kemp et al., 2002; Muhlbauer et al., 2012; Zalatan et al., 2001; Stumpf et al., 2008). Reduced melatonin levels are observed in various T2D rodent models and T2D patients (Peschke et al., 2006). Pinealectomy leads to reduced GLUT4 levels, glucose intolerance and insulin resistance (Lima et al., 1998; Nogueira et al., 2011). Upon administration of melatonin, glucose metabolism is improved in HFD induced insulin-resistant mouse model (Sartori et al., 2009). Several reports suggest the role of melatonin in insulin secretion and glucose uptake. In HepG2 cells, melatonin stimulates glycogen synthesis via protein kinase C, zeta (PKCζ), Akt and glycogen synthase kinase-3β (GSK3β) (Shieh et al., 2009) besides reducing gluconeogenesis in rats (Poon et al., 2001). The findings of melatonin regulating glucose metabolism via increased PI3K-Akt activity (Tuomi et al., 2016; Brydon et al., 2001) support our findings. Further, it is reported that melatonin activates IRS1–PI3K–PKCζ pathway and stimulates glucose uptake in mouse skeletal muscle cells (Ha et al., 2006), while it is reduced in MT1 knockout mice (Owino et al., 2018). In addition, melatonin is reported to inhibit lipolysis and fatty acid transport by inhibiting the cAMP–PKA pathway in rat adipocytes (Zalatan et al., 2001). Melatonin seems to have differential effects in the adipose tissue under acute and chronic treatments. Acute treatment inhibits cAMP and cGMP production in PAZ6 human brown adipocyte cell line, while chronic treatment reduces GLUT4 and glucose uptake (Brydon et al., 2001). In rodents, melatonin reduces body weight and white adipose tissue in various experimental models (Cipolla-Neto et al., 2014). A few small-scale clinical studies of melatonin treatment showed a negligible effect on body weight reduction with opposite results on plasma lipids (Karamitri

and Jockers, 2019). Furthermore, melatonin inhibits insulin secretion in rodent β-cells via Gi-cAMP-PKA (Muhlbauer et al., 2012; Karamitri et al., 2013; Peshchke et al., 2013) or cGMP pathway (Stumpf et al., 2008). However, long-term melatonin administration, increases insulin release in our study. Similar results are reported in INS-1 cells (Kemp et al., 2002; Peshchke et al., 2013). Acute melatonin treatment in clinical trials show impaired glucose tolerance (Cagnacci et al., 2001; Rubio- Sastre et al., 2014). However, chronic treatment of melatonin up to five months reduces HbA1c levels and hyperglycemia (Garfinkel et al., 2011). Human islet studies have shown increased intracellular Ca^{2+} levels and insulin incretion in β-cells (Ramracheya et al., 2008), possibly by paracrine signalling. Melatonin signalling promotes β-cell survival by decreasing apoptosis and oxidative stress in T2D patients' islets (Karamitri et al., 2013; Costes et al., 2015). These findings corroborate with our results, where β-cell mass increases along with insulin secretion. Similar to our findings, a combination study of melatonin and insulin also showed promising results in achieving glycemic control and insulin sensitivity in the adipose tissue as compared to the monotherapies (Oliveira et al., 2018). A very recent meta-analysis of randomized clinical trials investigating effects of melatonin supplementation on diabetes patients suggest that it reduces diabetes parameters like FBG, HbA1c levels, and insulin resistance (Delino et al., 2021).

Sitagliptin is the first approved DPP-IV inhibitor and is used widely for the management of T2D. DPP-IV plays an essential role in energy metabolism apart from its antidiabetic property (Goldsmith et al., 2015). Adipose tissue secretes DPP-IV, which impairs insulin signalling causing insulin resistance. Sitagliptin is a GLP-1 secretagogue that mediates its action via cAMP and ERK1/2 signalling (Sangle et al., 2012). Sitagliptin via GLP-1 promotes insulin signalling by increasing PKB (Akt) activity (Buteau et al., 2004; Li et al., 2005). In obese diabetic patients, leptin resistance causes increased leptin and insulin levels. We observed reduced leptin and insulin levels in all drug-treated groups showing the drugs involvement in lowering inflammatory markers. In this context, Dobrian et al. (2011) have reported the effect of sitagliptin in reducing local inflammation in adipose tissue and pancreatic islets in obese mice in addition to its insulin stimulatory effects.

Further, GLP-1 effects on adipocytes revealed its lipogenic and lipolytic functions (Villanueva-Penacarrillo et al., 2001; Vendrell et al., 2011) and, interestingly, the GLP-1 receptors in the white adipose tissue are structurally and functionally different from those in

the pancreas (Polakof et al., 2011). Sitagliptin treatment in diet-induced obesity reduces body weight (Lamont and Drucker, 2008). In clinical studies, similar results of reduced BW gain are seen in sitagliptin plus metformin-treated T2D patients (Raz et al., 2008; Bergenstal et al., 2010). Increasing GLP-1 levels reduces gluconeogenesis, promotes satiety and fat loss leading to insulin sensitivity (Green et al., 2006). It also controls metabolic abnormalities in HFD induced diabetic mice via peroxisome proliferator-activated receptor alpha (PPAR)-α activation in the liver (Souza-Mello et al., 2010). Our *in-vivo* studies are in agreement with these findings.

Furthermore, sitagliptin may slow down the progression of T2D by preserving β-cell mass, as observed by Yeom et al. (2011) in db/db mice. Our findings of increased β-cell mass seem to bring about glycemic control. However, it is essential to know if there is any different effect of sitagliptin on β-cell mass in lean subjects. We did not observe any significant change in food and water intake after sitagliptin treatment, as observed by Poucher et al. (2012). Nevertheless, we observed significant increase in insulin and glucose tolerance besides improved lipid profile, which supports studies by Akaslan et al. (2013) and Reimer et al. (2012), indicating improved lipid profile and insulin sensitivity in obese rats Thus, sitagliptin shows its therapeutic effects on glycolipid metabolism in T2D (Yang et al., 2016).

Interestingly, our study also reveals increased glycolysis, glycogen synthesis and glycogen content, and reduced gluconeogenesis, glycogenolysis and *GLUT2* expression in the liver, suggesting improved glucose metabolism in all drug-treated groups. Our mitochondrial studies suggest increased respiratory chain complexes I-IV activities in skeletal muscle in all drug treated groups. To our knowledge, there are no reports of the effects of sitagliptin treatment on mitochondrial function. However, Apaijai et al. (2013) showed improved cardiac mitochondrial function upon sitagliptin treatment in obese insulin-resistant rats. Defective insulin signalling leads to insulin resistance. Over nutrition causes activation of mTOR/S6K1 signalling and impairs insulin signalling by increased serine phosphorylation of IRS1 (Copps and White, 2012; Jia et al., 2014). A recent study showed decreased S6K1 activation and degradation of IRS1 and IRS2 upon sitagliptin treatment in obese mice (Qiao et al., 2018). We report a significant decrease in serine phosphorylation of IRS1 and increase in IR1β, pAKT and GLUT4 expression in all drug-treated groups. Sitagliptin activation of SIRT1- AMP-activated protein kinase (AMPK)/ adiponectin-AMPK/ PGC1-α-pAMPK pathway and downstream signalling are reported in liver, adipose tissue and skeletal muscle.

Such activation leads to modulation of fatty acid metabolism and further reduces insulin resistance in T2D models (Shen et al., 2018; Prakash et al., 2020; Liu et al., 2020).

Similarly, we have observed decrease in *ATGL* (lipolytic) transcript levels in adipose tissue with no change in *ACC1* (lipogenic) in all the drug-treated groups. In addition, increased *SIRT1* and *PGC1-α* (mitochondrial biogenesis genes) in the drug-treated groups in skeletal muscle, indicating improved lipid metabolism and insulin sensitivity in the respective tissues. *ACC1* helps in fatty acid (FA) synthesis in liver and adipose tissue. Moreover, reduced *ACC1* expression decreases TG accumulation (Mao et al., 2006), as also observed in our study. However, the decreased expression of *ACC1* in HFD group could be due compensation as the TG levels are significantly higher. Furthermore, our ddPCR results revealed increased expression of *MTNR1B, GLUT4* and *TNF-α* in HFD group indicating insulin resistance whereas the levels were decreased in all the drug treated groups signifying increased insulin sensitivity in adipose tissue. There are various reports which suggest that overexpression of *GLUT4* increases insulin sensitivity and glucose tolerance in HFD fed mice (Atkinson et al., 2013), and that its expression changes with short term and long term HFD feeding (Kim et al., 2014). It is possible that the overexpression was to compensate for insulin resistance in HFD group which was then reduced in all drug-treated groups showing increased insulin sensitivity. Moreover, *TNF-α,* a pro-inflammatory adipokine increases in obesity and T2D leading to insulin resistance (Patel et al., 2019). In addition, *MTNR1B* overexpression in adipose tissue leads to increased lipid levels in adipocytes (Owino et al., 2018) which is supported by our results showing increased TG levels and fat in HFD group while we observed decreased expression of *MTNR1B* expression and lipid levels in all drug-treated groups.

Thus, melatonin and sitagliptin in combination potentiate each other's action and improves glycolipid metabolism, insulin sensitivity, mitochondrial respiration and biogenesis, and preserves β-cell mass in HFD-induced T2D mouse model (Figure 5.10).

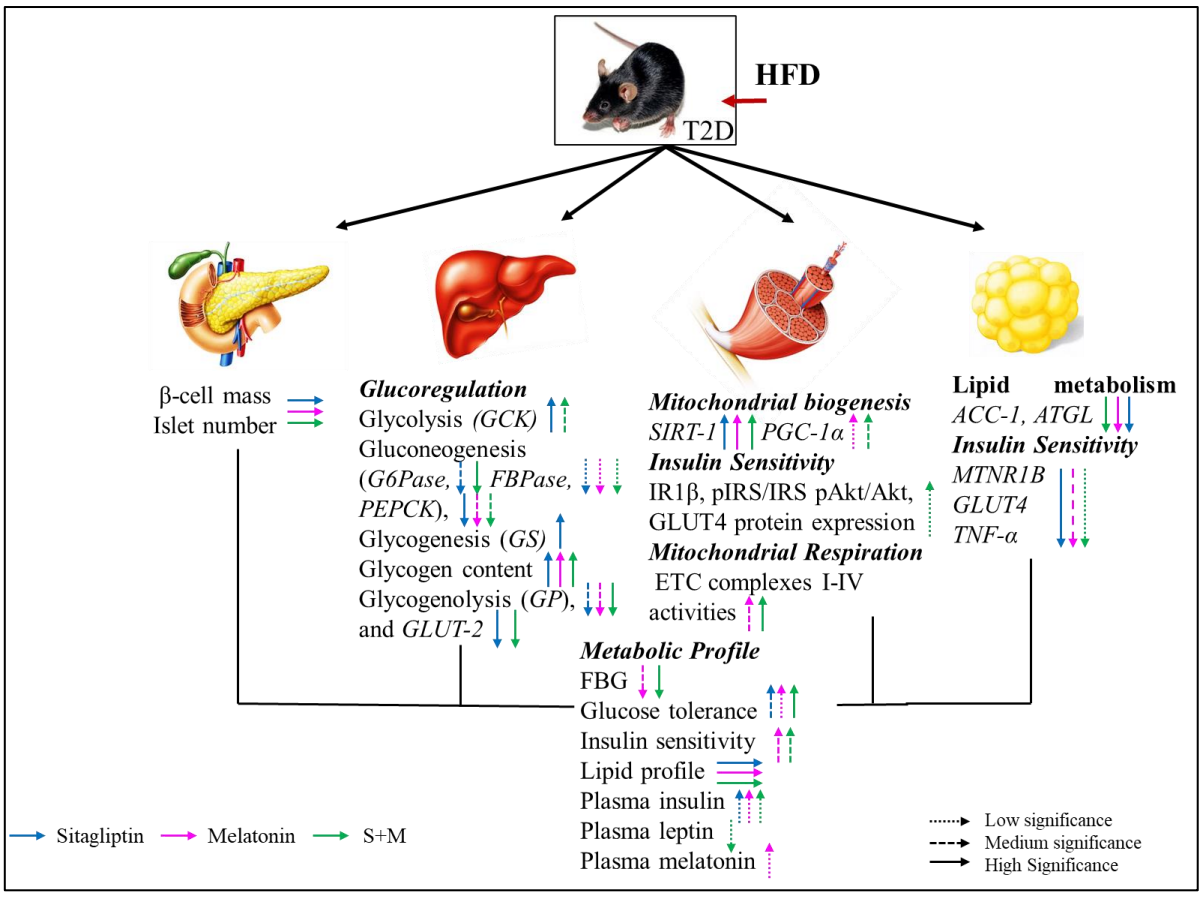

Figure 5.10 Effect of sitagliptin, melatonin, and combination therapy in amelioration of HFD-induced T2D manifestations in a mouse model. Combination of sitagliptin and melatonin shows greater therapeutic benefits than monotherapies in improving glyco-lipid metabolism in liver and adipose tissue, respectively; regulating mitochondrial biogenesis and mitochondrial respiration in skeletal muscle; increasing insulin sensitivity in skeletal muscle and adipose tissue; and maintaining β-cell mass and islet number in pancreas. These altogether brings about glucose homeostasis thereby ameliorating T2D manifestations.

As differences in the species play a significant role in influencing melatonin effects on glucose homeostasis, it is essential to consider acute/chronic melatonin treatment and paracrine interactions while translating its therapeutic effects in humans.

5.5 References

Akaslan SB, Degertekin CK, Yilmaz G, Cakir N, Arslan M, Toruner FB. Effects of sitagliptin on nonalcoholic fatty liver disease in diet-induced obese rats. Metab Syndr Relat Disord 2013;11(4):243-250.

Apaijai N, Pintana H, Chattipakorn SC, Chattipakorn N. Effects of vildagliptin versus sitagliptin, on cardiac function, heart rate variability and mitochondrial function in obese insulin-resistant rats. Br J Pharmacol 2013;169(5):1048-1057.

Atkinson BJ, Griesel BA, King CD, Josey MA, Olson AL. Moderate GLUT4 overexpression improves insulin sensitivity and fasting triglyceridemia in high-fat diet–fed transgenic mice. Diabetes 2013;62(7):2249-2258.

Bergenstal RM, Wysham C, MacConell L, et al. Efficacy and safety of exenatide once weekly versus sitagliptin or pioglitazone as an adjunct to metformin for treatment of type 2 diabetes (DURATION-2): a randomised trial. Lancet 2010;376(9739):431-439.

Bouatia-Naji N, Bonnefond A, Cavalcanti-Proença C, et al. A variant near MTNR1B is associated with increased fasting plasma glucose levels and type 2 diabetes risk. Nat Genet 2009;41(1):89-94.

Brydon L, Petit L, Delagrange P, Strosberg AD, Jockers R. Functional expression of MT2 (Mel1b) melatonin receptors in human PAZ6 adipocytes. Endocrinology 2001;142(10):4264-4271.

Buteau J, El-Assaad W, Rhodes CJ, Rosenberg L, Joly E, Prentki M. Glucagon-like peptide-1 prevents beta cell glucolipotoxicity. Diabetologia 2004;47(5):806-815.

Butterick TA, Stone LH, Duffy C, et al. Pioglitazone increases PGC1-α signaling within chronically ischemic myocardium. Basic Res Cardiol 2016;111(3):37.

Cagnacci A, Arangino S, Renzi A, et al. Influence of melatonin administration on glucose tolerance and insulin sensitivity of postmenopausal women. Clin Endocrinol 2001;54(3):339-346.

Cecon E, Oishi A, Jockers R. Melatonin receptors: molecular pharmacology and signalling in the context of system bias. Br J Pharmacol 2018;175(16):3263-3280.

Cipolla-Neto J, Amaral FG, Afeche SC, Tan DX, Reiter RJ. Melatonin, energy metabolism, and obesity: a review. J Pineal Res 2014;56(4):371-381.

Copps KD, White MF. Regulation of insulin sensitivity by serine/threonine phosphorylation of insulin receptor substrate proteins IRS1 and IRS2. Diabetologia 2012;55(10):2565-2582.

Costes S, Boss M, Thomas AP, Matveyenko AV. Activation of melatonin signaling promotes β-cell survival and function. Mol Endocrinol 2015;29(5):682-692.

de Oliveira AC, Andreotti S, Sertie RA, et al. Combined treatment with melatonin and insulin improves glycemic control, white adipose tissue metabolism and reproductive axis of diabetic male rats. Life Sci 2018;199:158-166.

Delpino FM, Figueiredo LM, Nunes BP. Effects of melatonin supplementation on diabetes: a systematic review and meta-analysis of randomized clinical trials. Clinical Nutrition. 2021;40(7):4595-4605.

Dobrian AD, Ma Q, Lindsay JW, et al. Dipeptidyl peptidase IV inhibitor sitagliptin reduces local inflammation in adipose tissue and in pancreatic islets of obese mice. Am J Physiol Endocrinol Metab 2011;300(2):E410-421.

Galano A, Tan DX, Reiter RJ. Melatonin as a natural ally against oxidative stress: a physicochemical examination. J Pineal Res 2011;51(1):1-6.

Garfinkel D, Zorin M, Wainstein J, Matas Z, Laudon M, Zisapel N. Efficacy and safety of prolonged-release melatonin in insomnia patients with diabetes: a randomized, double-blind, crossover study. Diabetes Metab Syndr Obes: Targets Ther. 2011;4:307.

Goldsmith F, Keenan MJ, Raggio AM, et al. Induction of energy expenditure by sitagliptin is dependent on GLP-1 receptor. PLoS One 2015;10(5):e0126177.

Green BD, Irwin N, Duffy NA, Gault VA, O'harte FP, Flatt PR. Inhibition of dipeptidyl peptidase-IV activity by metformin enhances the antidiabetic effects of glucagon-like peptide-1. Eur J Pharmacol. 2006;547(1-3):192-199.

Ha E, Yim SV, Chung JH, et al. Melatonin stimulates glucose transport via insulin receptor substrate-1/phosphatidylinositol 3-kinase pathway in C2C12 murine skeletal muscle cells. J Pineal Res 2006;41(1):67-72.

Herman GA, Bergman A, Stevens C, et al. Effect of single oral doses of sitagliptin, a dipeptidyl peptidase-4 inhibitor, on incretin and plasma glucose levels after an oral glucose tolerance test in patients with type 2 diabetes. J Clin Endocrinol Metab 2006;91(11):4612-4619.

Jia G, Aroor AR, Martinez-Lemus LA, Sowers JR. Overnutrition, mTOR signaling, and cardiovascular diseases. Am J Physiol Regul Integr Comp Physiol 2014;307(10):R1198-1206.

Kanter M, Uysal H, Karaca T, Sagmanligil HO. Depression of glucose levels and partial restoration of pancreatic β-cell damage by melatonin in streptozotocin-induced diabetic rats. Arch Toxicol 2006;80(6):362-369.

Karamitri A, Jockers R. Melatonin in type 2 diabetes mellitus and obesity. Nat Rev Endocrinol 2019;15(2):105-125.

Karamitri A, Renault N, Clement N, Guillaume JL, Jockers R. Minireview: Toward the establishment of a link between melatonin and glucose homeostasis: association of melatonin MT2 receptor variants with type 2 diabetes. Mol Endocrinol 2013;27(8):1217-1233.

Kemp DM, Ubeda M, Habener JF. Identification and functional characterization of melatonin Mel 1a receptors in pancreatic β cells: potential role in incretin-mediated cell function by sensitization of cAMP signaling. Mol Cell Endocrinol 2002;191(2):157-66.

Kim J, Jeong JI, Kim KM, Choi I, Pratley RE, Lee YH. Improved glucose tolerance with restored expression of glucose transporter 4 in C57BL/6 mice after a long period of high-fat diet feeding. Anim Cells Syst 2014;18(3):197-203.

Korkmaz A, Topal T, Tan DX, Reiter RJ. Role of melatonin in metabolic regulation. Rev Endocr Metab Disord 2009;10(4):261-270.

Lamont BJ, Drucker DJ. Differential antidiabetic efficacy of incretin agonists versus DPP-4 inhibition in high fat–fed mice. Diabetes 2008;57(1):190-198.

Li L, El-Kholy W, Rhodes CJ, Brubaker PL. Glucagon-like peptide-1 protects beta cells from cytokine-induced apoptosis and necrosis: role of protein kinase B. Diabetologia 2005;48(7):1339-1349.

Li Z, Graham BH. Measurement of mitochondrial oxygen consumption using a Clark electrode. In Mitochondrial Disorders 2012 (pp. 63-72). Humana Press.

Lima FB, Machado UF, et al. Pinealectomy causes glucose intolerance and decreases adipose cell responsiveness to insulin in rats. Am J Physiol Endocrinol Metab 1998; 275(6):E934-941.

Lin Y, Sun Z. Current views on type 2 diabetes. J Endocrinol. 2010;204(1):1.

Liu Y, Xu F, Jiang P. Effect of sitagliptin on expression of skeletal muscle peroxisome proliferator-activated receptor γ coactivator-1 α and irisin in a rat model of type 2 diabetes mellitus. J Int Med Res 2020;48(5):0300060519885569.

Mao J, DeMayo FJ, Li H, et al. Liver-specific deletion of acetyl-CoA carboxylase 1 reduces hepatic triglyceride accumulation without affecting glucose homeostasis. PNAS 2006;103(22):8552-7.

Mu J, Petrov A, Eiermann GJ, et al. Inhibition of DPP-4 with sitagliptin improves glycemic control and restores islet cell mass and function in a rodent model of type 2 diabetes. Eur J Pharmacol 2009;623(1-3):148-154.

Mu J, Woods J, Zhou YP, et al. Sitagliptin improves glycemic control and restores islet cell mass and function in a rodent model of type 2 diabetes. Diabetes 2007;56(Suppl 1):A550.

Mühlbauer E, Albrecht E, Bazwinsky-Wutschke I, Peschke E. Melatonin influences insulin secretion primarily via MT1 receptors in rat insulinoma cells (INS-1) and mouse pancreatic islets. J Pineal Res. 2012;52(4):446-459.

Nduhirabandi F, Du Toit EF, Blackhurst D, Marais D, Lochner A. Chronic melatonin consumption prevents obesity-related metabolic abnormalities and protects the heart against myocardial ischemia and reperfusion injury in a prediabetic model of diet-induced obesity. J Pineal Res 2011;50(2):171-82.

Nishida S, Sato R, Murai I, Nakagawa S. Effect of pinealectomy on plasma levels of insulin and leptin and on hepatic lipids in type 2 diabetic rats. J Pineal Res 2003;35(4):251-256.

Nishida S, Segawa T, Murai I, Nakagawa S. Long-term melatonin administration reduces hyperinsulinemia and improves the altered fatty-acid compositions in type 2 diabetic rats via the restoration of Δ-5 desaturase activity. J Pineal Res 2002;32(1):26-33.

Nogueira TC, Lellis-Santos C, Jesus DS, et al. Absence of melatonin induces night-time hepatic insulin resistance and increased gluconeogenesis due to stimulation of nocturnal unfolded protein response. Endocrinology 2011;152(4):1253-1263.

Oishi A, Cecon E, Jockers R. Melatonin receptor signaling: impact of receptor oligomerization on receptor function. Int Rev Cell Mol Biol 2018;338:59-77.

Owino S, Sánchez-Bretaño A, Tchio C, et al. Nocturnal activation of melatonin receptor type 1 signaling modulates diurnal insulin sensitivity via regulation of PI 3K activity. J Pineal Res 2018;64(3):e12462.

Pan M, Song YL, Xu JM, Gan HZ. Melatonin ameliorates nonalcoholic fatty liver induced by high-fat diet in rats. J Pineal Res 2006;41(1):79-84.

Patel R, Palit SP, Rathwa N, Ramachandran AV, Begum R. Genetic variants of tumor necrosis factor-α and its levels: A correlation with dyslipidemia and type 2 diabetes susceptibility. Clin Nutr 2019;38(3):1414-1422.

Patel R, Pramanik S, Rathwa NN, et al. 112-LB: Melatonin and DPP-IV Inhibitor: A Novel Combinatorial Approach for ß-Cell Regeneration. Diabetes 2019; (Suppl 1).

Patel R, Rathwa N, Palit SP, Ramachandran AV, Begum R. Association of melatonin & MTNR1B variants with type 2 diabetes in Gujarat population. Biomed Pharmacother 2018;103:429-434.

Peschke E, Bähr I, Mühlbauer E. Melatonin and pancreatic islets: interrelationships between melatonin, insulin and glucagon. Int J Mol Sci 2013;14(4):6981-7015.

Peschke E, Frese T, Chankiewitz E, et al. Diabetic Goto Kakizaki rats as well as type 2 diabetic patients show a decreased diurnal serum melatonin level and an increased pancreatic melatonin-receptor status. J Pineal Res 2006;40(2):135-143.

Peschke E, Mühlbauer E. New evidence for a role of melatonin in glucose regulation. Best Pract Res Clin Endocrinol Metab 2010;24(5):829-841.

Peschke E. Melatonin, endocrine pancreas and diabetes. J Pineal Res 2008;44(1):26-40.

Polakof S, Miguez JM, Soengas JL. Evidence for a Gut–Brain Axis Used by Glucagon-like Peptide-1 to Elicit Hyperglycaemia in Fish. J Neuroendocrinol 2011;23(6):508-518.

Poon AM, Choy EH, Pang SF. Modulation of blood glucose by melatonin: a direct action on melatonin receptors in mouse hepatocytes. Neurosignals 2001;10(6):367-379.

Poucher SM, Cheetham S, Francis J, Zinker B, Kirby M, Vickers SP. Effects of saxagliptin and sitagliptin on glycaemic control and pancreatic β-cell mass in a streptozotocin-induced mouse model of type 2 diabetes. Diabetes Obes Metab 2012;14(10):918-926.

Prakash S, Rai U, Kosuru R, Tiwari V, Singh S. Amelioration of diet-induced metabolic syndrome and fatty liver with Sitagliptin via regulation of adipose tissue inflammation and hepatic Adiponectin/AMPK levels in mice. Biochimie 2020;168:198-209.

Prokopenko I, Langenberg C, Florez JC, et al. Variants in MTNR1B influence fasting glucose levels. Nat Genet 2009;41(1):77-81.

Qiao S, Mao G, Li H, et al. DPP-4 inhibitor sitagliptin improves cardiac function and glucose homeostasis and ameliorates β-cell dysfunction together with reducing S6K1 activation and IRS-1 and IRS-2 degradation in obesity female mice. J Diabetes Res 2018;2018.

Ramracheya RD, Muller DS, Squires PE, et al. Function and expression of melatonin receptors on human pancreatic islets. J Pineal Res 2008;44(3):273-279.

Raz I, Chen Y, Wu M, et al. Efficacy and safety of sitagliptin added to ongoing metformin therapy in patients with type 2 diabetes. Curr Med Res Opin 2008;24(2):537-550.

Reimer RA, Grover GJ, Koetzner L, et al. Sitagliptin reduces hyperglycemia and increases satiety hormone secretion more effectively when used with a novel polysaccharide in obese Zucker rats. J Nutr 2012;142(10):1812-1820.

Reutrakul S, Hood MM, Crowley SJ, Morgan MK, Teodori M, Knutson KL, Van Cauter E. Chronotype is independently associated with glycemic control in type 2 diabetes. Diabetes Care 2013;36(9):2523-2529.

Ríos-Lugo MJ, Cano P, Jiménez-Ortega V, et al. Melatonin effect on plasma adiponectin, leptin, insulin, glucose, triglycerides and cholesterol in normal and high fat–fed rats. J Pineal Res 2010;49(4):342-348.

Rubio-Sastre P, Scheer FA, Gómez-Abellán P, Madrid JA, Garaulet M. Acute melatonin administration in humans impairs glucose tolerance in both the morning and evening. Sleep 2014;37(10):1715-1719.

Sakura H, Hashimoto N, Sasamoto K, et al. Effect of sitagliptin on blood glucose control in patients with type 2 diabetes mellitus who are treatment naive or poorly responsive to existing antidiabetic drugs: the JAMP study. BMC Endocr Disord 2016;16(1):1-1.

Sangle GV, Lauffer LM, Grieco A, Trivedi S, Iakoubov R, Brubaker PL. Novel biological action of the dipeptidylpeptidase-IV inhibitor, sitagliptin, as a glucagon-like peptide-1 secretagogue. Endocrinology 2012;153(2):564-573.

Sartori C, Dessen P, Mathieu C, et al. Melatonin improves glucose homeostasis and endothelial vascular function in high-fat diet-fed insulin-resistant mice. Endocrinology 2009;150(12):5311-5317.

Scheer FA, Hilton MF, Mantzoros CS, Shea SA. Adverse metabolic and cardiovascular consequences of circadian misalignment. PNAS 2009;106(11), 4453-4458.

Shen T, Xu B, Lei T, Chen L, Zhang C, Ni Z. Sitagliptin reduces insulin resistance and improves rat liver steatosis via the SIRT1/AMPKα pathway. Exp Ther Med 2018;16(4):3121-8.

Shieh JM, Wu HT, Cheng KC, Cheng JT. Melatonin ameliorates high fat diet-induced diabetes and stimulates glycogen synthesis via a PKCζ-Akt-GSK3β pathway in hepatic cells. J Pineal Res 2009;47(4):339-344.

Souza-Mello V, Gregorio BM, Cardoso-de-Lemos FS, de Carvalho L, Aguila MB, Mandarim-de-Lacerda CA. Comparative effects of telmisartan, sitagliptin and metformin alone or in combination on obesity, insulin resistance, and liver and pancreas remodelling in C57BL/6 mice fed on a very high-fat diet. Clin Sci. 2010;119(6):239-250.

Stoscheck CM. [6] Quantitation of protein. Meth. Enzymol 1990;182:50-68.

Stumpf I, Mühlbauer E, Peschke E. Involvement of the cGMP pathway in mediating the insulin-inhibitory effect of melatonin in pancreatic β-cells. J Pineal Res 2008;45(3):318-327.

Tuomi T, Nagorny CL, Singh P, et al. Increased melatonin signaling is a risk factor for type 2 diabetes. Cell Metab. 2016;23(6):1067-1077.

Vendrell J, El Bekay R, Peral B, et al. Study of the potential association of adipose tissue GLP-1 receptor with obesity and insulin resistance. Endocrinology 2011;152(11):4072-4079.

Villanueva-Penacarrillo ML, Marquez L, Gonzalez N, Diaz-Miguel M, Valverde I. Effect of GLP-1 on lipid metabolism in human adipocytes. Horm Metab Res. 2001;33(02):73-77.

Yang J, Ba T, Chen L, et al. Effects of metformin and sitagliptin on glycolipid metabolism in type 2 diabetic rats on different diets. Arch Med Sci: AMS 2016;12(2):233.

Yeom JA, Kim ES, Park HS, et al. Both sitagliptin analogue & pioglitazone preserve the β-cell proportion in the islets with different mechanism in non-obese and obese diabetic mice. BMB Rep 2011;44(11):713-718.

Zalatan F, Krause JA, Blask DE. Inhibition of isoproterenol-induced lipolysis in rat inguinal adipocytes in vitro by physiological melatonin via a receptor-mediated mechanism. Endocrinology 2001;142(9):3783-3790.